In-line liquid-crystal microcell wave plates and their application for high-speed, reset-free polarization mode dispersion compensation in 40-Gbit/s systems

Bharat R. Acharya, Lothar Möller, Kirk W. Baldwin, Robert A. MacHarrie, Ray A. Stepnoski, Cheng C. Huang, Ron Pindak, and John A. Rogers

We describe the design, fabrication, and performance of a high-speed, continuously tunable, and reset-free polarization controller based on nematic liquid-crystal (NLC) microcell wave plates fabricated directly between the tips of optical fibers. This controller utilizes a pulsed driving scheme and optimized NLC materials to achieve a stepwise switching speed of 1 deg/μs, for arbitrary rotation angles with moderately low voltages. This compact microcell design requires no bulk optical components and has the potential to have low insertion loss. We describe the performance of these devices when implemented in polarization mode dispersion compensators for 40 Gbit/s systems. The good optical properties and the nonmechanical, high-speed, and low-power operation suggest that this type of device might be considered for some applications in dynamic compensation of polarization mode dispersion, polarization analysis, polarization division demultiplexing, and polarization scrambling in high-speed optical communication systems.

OCIS codes: 060.0060, 350.0350, 160.3710.

1. Introduction

Recent developments in high-speed wavelength division multiplexed communication systems have created an interest in devices for high-performance polarization management, such as polarization mode dispersion (PMD) compensation[1] and polarization division multiplexing.[2] Differential group delay (DGD) between orthogonal polarization modes introduces PMD that must be compensated in fiber-optic communication systems with high per-channel data transmission rates (above 10 Gbits/s). In general, PMD fluctuations are random and they vary with time and wavelength in a way that must be compensated dynamically on a per-channel basis in a cost-effective way. One approach uses a polarization controller (PolCon), which transforms an arbitrary input state of polarization (SOP) to an arbitrary output SOP, and a static high-birefringence optical fiber in front of the receiver.[1] The PolCon transforms the input SOP to the eigenstate of the high-birefringence fiber which, in turn, compensates for the DGD introduced in the optical signal. The PMD fluctuations are typically in the acoustic frequency range (<10 kHz). However, the dynamic monitoring and feedback needed for PMD compensation requires a much faster (~1-μs) switching speed for the PolCon. PolCons based on different technologies such as fiber squeezers,[3] $LiNbO_3$,[4] and liquid crystals[5–7] have been demonstrated. Liquid-crystal (LC)-based devices offer some advantages because of their nonmechanical, low-power operation, their ease of fabrication, and their potential to have low loss and be inexpensive.

PolCons based on variable-birefringence nematic liquid crystals (NLCs) reported earlier[5] have a finite tuning range and hence require complicated resetting algorithms. Devices based on rotatable NLC wave plates[6] avoid this problem, but previous designs

B. R. Acharya (bacharya@lucent.com), K. W. Baldwin, R. A. MacHarrie, R. A. Stepnoski, and J. A. Rogers are with Bell Laboratories, Lucent Technologies, Murray Hill, New Jersey 07974. L. Möller is with Bell Laboratories, Lucent Technologies, Holmdel, New Jersey 07733. C. C. Huang is with the School of Physics and Astronomy, University of Minnesota, Minneapolis, Minnesota 55455. R. Pindak is with the National Synchrotron Light Source, Brookhaven National Laboratory, Upton, New York 11973.

Received 14 February 2003; revised manuscript received 22 May 2003.

0003-6935/03/275407-06$15.00/0

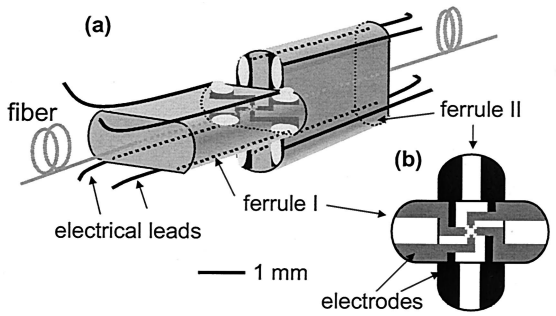

Fig. 1. (a) Schematic diagram of the fiber ferrule based microcell wave plate. (b) Top view of the wave plate.

required large numerical aperture bulk optics to collimate and to focus light and have millisecond switching speeds. Although rotatable wave plates based on electroclinic materials have been reported to operate with microsecond switching speeds,[7] the thickness required for efficient modulation is large [e.g., ~40 μm for a half-wave plate (HWP)]. Nonuniformities in the electric field and imperfect LC alignment through these thick cells represent some limitations for this type of device. Here we report the design, fabrication, and performance of a reset-free NLC PolCon that utilizes microcell wave plates formed with microelectrodes patterned directly on the tips of optical fibers. In a pulsed-mode operation, this device is capable of microsecond switching speeds, and it shows other attractive optical characteristics when implemented for PMD compensation in 40 Gbit/s systems.

2. Design and Fabrication

Fabrication of the liquid-crystal microcell wave plate begins with photolithographic patterning of two pairs of 0.2-μm-thick gold electrodes on the end facet of a fiber mounted in a flat glass ferrule. The core of the fiber lies at the center of the electrodes, which are each 5 μm wide and spaced 25 μm apart. Rotating two such ferrules by 90° and aligning them with a predetermined spacing forms the microcell wave plate. The alignment of these fiber ferrules was done manually by use of conventional translation stages with micrometer precision in a similar fashion as is usually done in coupling single-mode fibers to waveguide devices. Figure 1(a) shows the schematic of the assembly. A top view of the electrode arrangement is depicted in Fig. 1(b). The electrodes that are directly opposite each other on the two ferrules were connected together and an electric potential $V_i(\phi) = V_0 \cos(i*90 + \phi)$ was then applied to the ith electrode. V_0 is a 10-kHz square wave with a 100-V peak amplitude. These applied voltages control azimuthal orientation ϕ of the optic axis of a NLC layer that is loaded by capillary action into the gap between the fibers. The devices described here use NLC MLC-14200-000 (Merck Chemicals), which has a large optical birefringence ($\Delta n \approx 0.10$ at $\lambda = 1.55$ μm), high dielectric anisotropy ($\Delta\epsilon = 29.3$), relatively low rotational viscosity ($\gamma_1 = 297$ mPa at 20 °C), and a high nematic–isotropic transition temperature ($T_{N-I} = 95$ °C). Calculations and quantitative analysis of the experimental results obtained by rotation of the optic axis of the LC layer showed that, for this NLC, the thickness required for a quarter-wave plate (QWP) and a HWP are ~4 and ~8 μm, respectively.[8] Since the PolCons, in general, are used for continuous tracking and analysis of the input SOP, the microcell wave plates are operated with the field magnitude at a constant and relatively large value. In this high-field regime, the possible misalignment of the director at the thin LC–glass interface has a negligible effect on the overall optic axis orientation. Therefore, we did not apply any alignment layer, which simplifies the fabrication process and avoids some of the long-term reliability challenges associated with changes that can occur in many types of polymer alignment film.

3. Results

A uniform orientation and switching of the optic axis of the NLC layer requires an electric field that is uniform both in magnitude and direction. For in-plane electrodes, the uniformity of the field depends on the electrode width and thickness, their separation, and cell thickness. Figure 2 shows a photomicrograph of the electrodes on the fiber tip and computed electric-field distributions for this configuration; these results were obtained by numerically solving the three-dimensional Laplace equation with appropriate boundary conditions. Figure 2(b) depicts the variation of the magnitude of the in-plane component of the electric field in the midplane between the two substrates for $\phi = 0°$. Figure 2(c) shows the cosine square of the angular deviation from $\phi = 0°$. These results show that the orientation of the field is uniform in the central region of ~12-μm diameter to within ~5%. Thus, if the active area of the device is small, such as in a single-mode optical fiber, where the mode field diameter is ~10 μm, the electrodes can be brought close to each other and still maintain a uniform electric field over the area where the optical intensity is significant. This approach minimizes the operating voltages. We also note that the four-electrode design, which is simpler than the eight-electrode layout reported earlier for a bulk cell,[6] provides an electric field that shows good uniformity over the active area.

The switching speed of NLC material depends on dielectric anisotropy and rotational viscosity of the material, operating temperature, and strength of the driving electric field. We exploited all these parameters to achieve higher switching speed than in conventional devices. Moreover, for the in-plane switching in conventional devices, the speed also depends on the relative orientation of the electric field with respect to the initial orientation of the nematic director. Since the torque that acts on the director at smaller angles is lower, the switching time does not scale linearly with angles, i.e., a continuous rotational speed of 45° in 45 μs does not correspond to a discrete rotation of 1° in 1 μs. We developed a driv-

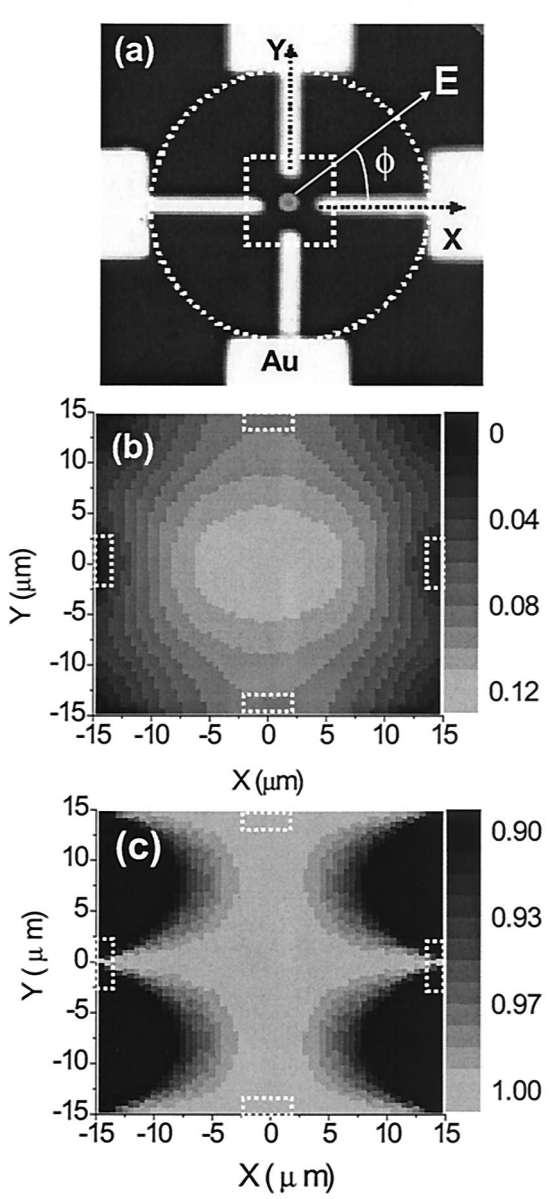

Fig. 2. (a) Electrode structure at the tip of the ferrule. The circle represents the perimeter of the 125-μm-diameter single-mode fiber and the dot at the center represents its core. The square at the center depicts the base of the 5-μm-thick box used in the calculation of the in-plane component of electric field E in the midplane between two substrates for $\phi = 0°$. (b) The magnitude of the in-plane component of the electric field. (c) The cosine square of the angular deviation of the field. The dotted lines represent the location of the electrodes on the substrate plane. The anisotropy of the dielectric constant of the LC was neglected in these calculations.

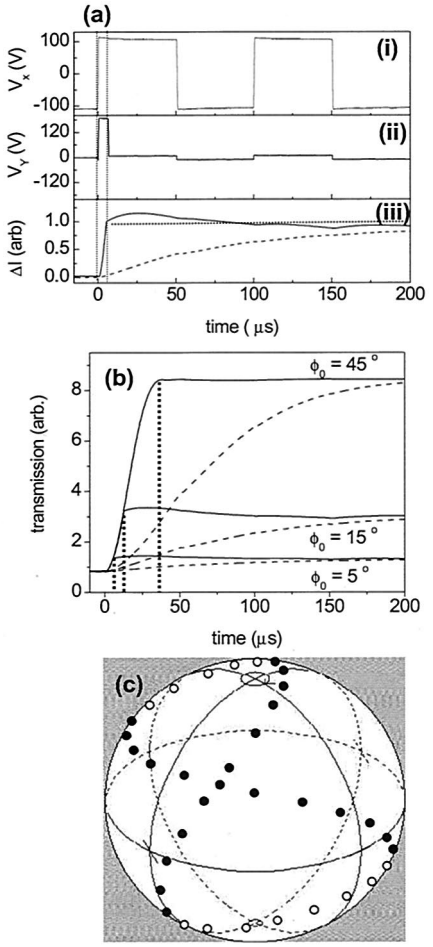

Fig. 3. (a) Potentials (i) and (ii) applied to x and y electrodes, respectively. At time $t = 0$, the potentials were switched from the values required to orient the director at $\phi = 0$ to $\phi = 5°$. (iii) Change in optical intensity ΔI at the photodetector when the director rotates through 5° with (solid curve) and without (dashed curve) a triggering pulse. The vertical dotted lines represent the time during which a stronger pulse directed along 60° was applied. (b) Switching characteristics for a fiber ferrule based NLC QWP for various angular orientations with (solid curves) and without (dashed curves) the triggering pulse oriented at 60°. The vertical dashed lines show the corresponding switching times. (c) Evolution of the SOP of linearly polarized light when the optic axis of the QWP is rotated by 180°. The filled (open) circles represent the front (back) of the Poincaré sphere. The slight asymmetry and the tilt in the figure-8 contour are due to the fiber segments between the source and the LC layer and the LC layer and the detector.

ing scheme to overcome this problem by applying a pulsed electric field oriented at larger angles to provide stronger torque for smaller angular rotation. Large torque exerted on the director in the beginning rotates the director faster through smaller angles compared with when the director is rotated only through the smaller angle. This driving approach allows a discrete rotational speed of 1 deg/μs at moderately low applied voltage. Light at 1.55-μm wavelength from a laser source was launched to the NLC QWP, and the signal was detected at a photodetector placed after a polarizer. We then rotated the optic axis of the QWP through different azimuthal angles by rotating the electric field, and we recorded the switching time responses of the device. Figure 3(a) depicts the applied potentials to x and y electrodes and the change in the optical intensity when the optic axis of the QWP was rotated by 5° at room temperature by use of $V_0 = 100V_p$ with and without a trig-

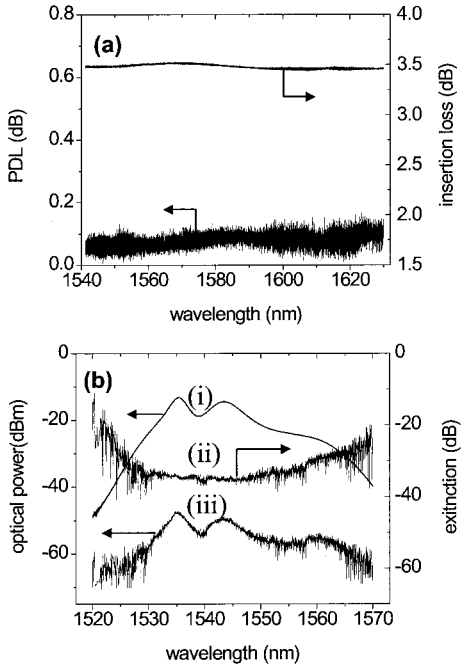

Fig. 4. (a) Insertion loss and the polarization-dependent loss of the NLC PolCon in the C and L bands. (b) ASE spectra when the NLC PolCon was adjusted for (i) maximum and (iii) minimum transmission between the crossed polarizers. Spectrum (ii) is the difference between (i) and (iii).

gering pulse ($V_t = 200V_p$) directed at 60°. Figure 3(b) depicts the switching characteristics for various azimuthal orientations with and without the triggering pulse directed at 60°. Clearly, the switching speed improves significantly compared with that without a triggering pulse. We obtained comparable speed with V_t the same as V_0 by raising the operating temperature to ~75 °C.[9] Figure 3(c) shows the evolution of the SOP of a linearly polarized light as the optic axis of the QWP is rotated. The slight asymmetry and the tilt in the figure-8 contour is due to the slight modification of the SOP of the light due to the segments of the fiber between the source and the LC layer and the LC layer and the analyzer. By gluing a 30-μm-thick Polarcor UltraThin (Corning, Inc.) polarizer onto the tip of the optical fiber in front of the LC layer and canceling the effect of the fiber between the LC layer and the detector, we obtained the perfect figure-8 contour as expected for a rotating QWP.[10] A quantitative analysis of the intensity observed after an analyzer yielded a phase retardation of 91.6°.[8]

In general, any arbitrary input SOP can be transformed to any arbitrary output SOP by insertion of a HWP between two QWPs and adjustment of the azimuthal orientations of the optic axes of these wave plates.[11] Two microcell QWPs with a microcell HWP between them, all with the design described above, were connected together in series with conventional fiber splices to form a continuously tunable, endlessly rotatable PolCon. Figure 4(a) depicts the insertion loss and polarization-dependent loss of this

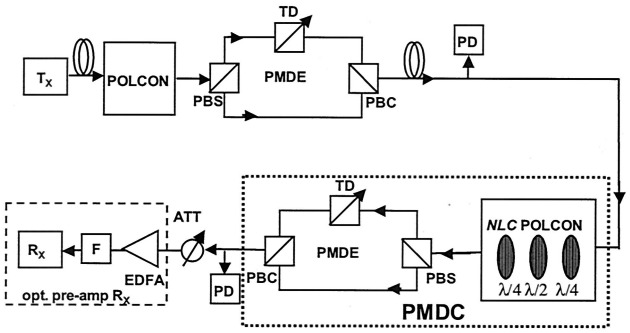

Fig. 5. Experimental setup for the PMD compensation in a 40-Gbit/s optical transmission system. T_x, transmitter; PBS, polarization beam splitter; TD, tunable delay; PMDE:PMD emulator; PBC, polarization beam combiner; PD, photodetector; PMDC, PMD compensator; ATT, optical attenuator; EDFA, erbium-doped fiber amplifier; F, optical filter; R_x, receiver.

device over the spectrum of an amplified stimulated emission (ASE) light source. Clearly, both the insertion loss and the polarization-dependent loss are almost constant over the entire C and L bands at 3.5 and 0.1 dB, respectively. Since the total thickness of the LC layer is less than 20 μm and the absorption of the signal by the NLC layer is negligible, calculations show that the insertion loss for the three microcell wave plates could be as low as 0.3 dB.[7] The experimentally achieved insertion loss comes mainly from splice losses and potentially from angular and/or transverse misalignment of fiber cores during packaging. Both sources of loss can be reduced significantly by fusion splicing and efficient packaging.

Even when the length and the bend of the single-mode fiber between the wave plates are minimized, these connecting fibers can transform the SOP in a nontrivial fashion. We employed a crossed polarizer test[12] to evaluate further the performance of the PolCon. The device was placed between a polarization converter (consisting of a polarizer, a QWP, and a HWP) and a polarizer. An ASE with a broadband spectrum was used as the optical source. The signal from the polarizer was then fed to an optical spectrum analyzer. We launched three different SOPs (an orthogonal set as viewed on the Poincaré sphere: two linearly polarized states separated by 90° on the azimuth and a right circularly polarized state) by adjusting the azimuthal orientations of the wave plates in the polarization converter, and the NLC PolCon was adjusted to attenuate the input signal to the optical spectrum analyzer. For all three SOPs, by using the NLC PolCon, we were able to attenuate the signal by more than 30 dB over a wide wavelength range (>30 nm) around 1550 nm. Since any polarization state can be expressed in terms of these three SOPs, we can infer that the PolCon was able to transform any arbitrary polarization state to any arbitrary polarization state. Figure 4(b) shows the actual spectrum of the source and the spectrum after attenuation by the LC PolCon for one of the SOPs.

The NLC PolCon causes no intrinsic signal distor-

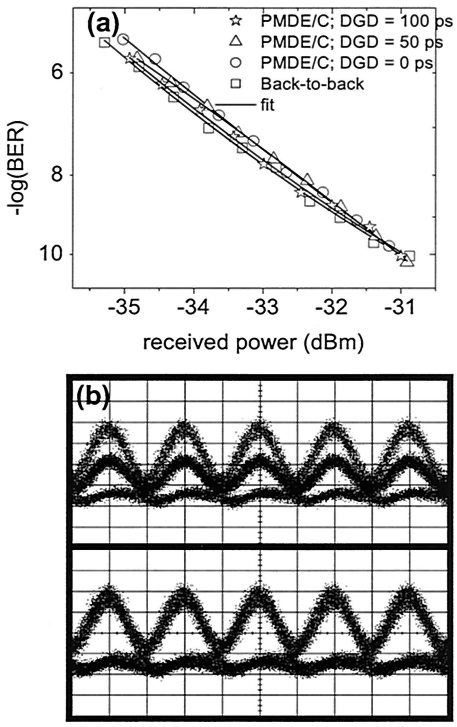

Fig. 6. (a) Receiver sensitivity after PMD compensation compared with the back-to-back operation (no PMD, without NLC PolCon) in a 40-Gbit/s 33% return-to-zero transmission system for different amounts of DGD. (b) Eye diagrams for 100-ps DGD before PMD compensation (top) and after PMD compensation (bottom).

tions such as pulse shape deformation. We demonstrate this characteristic by superposing the data signal in a 40-Gbit/s test-bed system with optical noise and then measuring the bit error ratio (BER) curves at an optically preamplified receiver. For these system tests, a single-stage PMD compensator was built by combining the NLC PolCon with a tunable DGD element. Figure 5 is a schematic diagram of the experimental setup. We first distorted a 40-Gbit/s 33% return-to-zero signal from the transmitter by introducing first-order PMD by use of a tunable PMD emulator. The PMD emulator consists of a polarization beam splitter that splits the incoming signal into two equal orthogonal polarization states that propagate along optical paths, a tunable delay line in one of the paths, and a polarization beam combiner that combines two polarization states. By adjusting the SOP of the incoming signal using a conventional PolCon (POLCON in Fig. 5), we split the incoming signal into two equal orthogonal components. Adjustment of the time delay on one of the paths allowed introduction of various amounts of PMD to distort the signal. The distorted signal was then launched into a first-order PMD compensator that consisted of a NLC PolCon and a DGD element similar to the PMD emulator. We adjusted the PMD compensator manually such that the BER was minimized.

For different amounts of PMD introduced, we measured the sensitivity of an optically preamplified receiver. Figure 6(a) shows variation of the BER as a function of the input power to the optical preamplifier. By reducing the launched power to the erbium-doped fiber amplifier we added more ASE noise to the signal in the preamplifier. Any kind of pulse shape distortion would be visible as performance degradation with an increase in the required preamplifier input power for a minimum BER. The insertion loss of the PolCon does not appear in the measurement curves since the preamplifier input power versus the BER is recorded. The sensitivity curves of the equalized signals show no remaining penalty (within 0.2-dB measurement accuracy). Figure 6(b) shows the eye diagram when the 100-ps DGD was introduced in the system before (top) and after (bottom) PMD compensation. This demonstrates that the NLC PolCon can be used in high-speed transmission without causing additional signal distortion.

4. Summary

We have developed a PolCon based on NLC microcell wave plates fabricated directly between the tips of optical fibers. A switching speed of 1 deg/μs was demonstrated with these devices at moderately low operating voltages. The PolCon is capable of transforming any arbitrary input SOP to any arbitrary output SOP with reset-free operation. Although the observed insertion loss is not at the theoretical minimum, it can be reduced significantly by efficient alignment and packaging of the fiber ferrule assemblies. This PolCon shows no signal distortion when implemented in PMD compensation in 40-Gbit/s system tests. Our current research focuses on implementing this device for dynamic PMD compensation and related polarization management systems.

This research was partially funded by the National Science Foundation Grant Opportunities for Academic Liason with Industry project. The authors acknowledge the stimulating discussion with P. Westbrook of OFS/Fitel Laboratory and the technical assistance of E. Chaban. We also acknowledge J. Pitney for his help in fabricating and testing early prototypes of the device.

References

1. C. D. Poole and J. Nagel, "Polarization effects in lightwave systems," in *Optical Fiber Telecommunications IIIA*, I. P. Kaminow and T. L. Koch, eds. (Academic, San Diego, Calif., 1997), pp. 114–162.
2. K. Fukuchi, T. Kasamatsu, M. Morie, R. Ohhira, T. Ito, K. Sekiya, D. Ogasahara, and T. Ono, "10.92-tb/s (273 × 40 Gb/s) triple-band/ultra dense WDM optical-repeated transmission experiment," in *Optical Fiber Communication Conference*, Vol. 54 of OSA Trends in Optics and Photonics (Optical Society of America, Washington, D.C., 2001), postdeadline paper PD24–1.
3. H. Shimizu, S. Yamazaki, T. Ono, and K. Imura, "Highly practical fiber squeezer polarization controller," J. Lightwave Technol. **9,** 1217–1224 (1991).
4. F. Heismann and M. S. Whalen, "Fast automatic polarization

control system," IEEE Photon. Technol. Lett. **4,** 503–505 (1992).
5. K. Hirabayashi and C. Amano, "Liquid-crystal polarization controller arrays on planar waveguide circuits," IEEE Photon. Technol. Lett. **14,** 504–506 (2002).
6. T. Chiba, Y. Ohtera, and S. Kawakami, "Polarization stabilizer using liquid crystal rotatable waveplates," J. Lightwave Technol. **17,** 885–890 (1999).
7. L. Dupont, J. L. de Bougrenet de la Tocnaye, M. Le Gall, and D. Penninckx, "Principle of a compact polarization mode dispersion controller using homeotropic electronic liquid crystal confined single mode fiber devices," Opt. Commun. **176,** 113–119 (2000).
8. B. R. Acharya, C. K. Madsen, K. W. Baldwin, R. A. MacHarrie, J. A. Rogers, L. Möller, C. C. Huang, and R. Pindak, "In-fiber nematic liquid crystal optical modulator based on in-plane switching with microsecond response time," Opt. Lett. **28,** 1096–1098 (2003).
9. B. R. Acharya, K. W. Baldwin, R. A. MacHarrie, J. A. Rogers, C. C. Huang, and R. Pindak, "High speed liquid crystal optical modulator based on in-plane switching," Appl. Phys. Lett. **81,** 5243–5246 (2002).
10. R. M. A. Azzam, "Poincaré sphere representation of the fixed-polarizer rotating-retarder optical system," J. Opt. Soc. Am. A **17,** 2105–2107 (2000).
11. P. Yeh and C. Gu, *Optics of Liquid Crystal Displays* (Wiley, New York, 1999), pp. 38–39.
12. See, for example, Ref. 1, p. 150.